10th World Congress on Structural and Multidisciplinary Optimization
May 19 -24, 2013, Orlando, Florida, USA

Optimization of Effective Diffusivity by Iso-surface Modeling

Che-Cheng Chang[1], Shiwei Zhou[2] and Qing Li[1]

[1] School of Aerospace, Mechanical and Mechatronic Engineering, The University of Sydney, Sydney, NSW 2006, Australia, checheng.chang@sydney.edu.au
[2] Centre for Innovative Structures and Materials, School of Civil, Environmental and Chemical Engineering, RMIT University, GPO Box 2476, Melbourne 3001, Australia,

1. Abstract
In tissue engineering, cell survival in porous tissue scaffolds relies on efficient and sustained oxygen transport, which is especially important in static scaffolding conditions. However, cell deposition and proliferation can impose physical barriers to both mass transport and the diffusion of oxygen, thus affect the uniformity of oxygen concentration across the entire scaffold construct. This can then potentially lead to the regional hypoxia and cell death. The goal of this study is to optimize the periodic microstructure of scaffold to allow the maximum effective diffusivity, which in turn provides the ideal environment for nutrient transportation in porous medium. In this study, homogenization and level set optimization are performed to determine the effective diffusivity and track the evolution of microstructure, respectively. Considering the boundary sensitivity in such fluidic problems, the isosurface modeling was implemented to improve the solution quality. The optimal microstructure has been obtained and characterized by the roughly uniform-width gap space for diffusion, and the smooth solid-fluid boundary. These features significantly improve the accessibility of space to diffusion flux in multiple directions. Such space-sharing characteristic is evidently the key to achieve the highest volume-effectiveness for diffusion transport. The final result with the maximized diffusivity can be applied to tissue scaffolds to improve the cell survival and proliferation rate.

2. Keywords: Level set optimization; effective diffusivity; isosurface; porous tissue scaffold.

3. Introduction
Poor cell growth in tissue scaffolds is commonly attributed to insufficient oxygen supply [1, 2]. Cell distribution deviation [3] and shallow infiltration [4, 5] are typical results of the failure to sustain the required oxygen concentration level across the entire tissue scaffold, especially in a static condition. This oxygen and nutrient transportation problem represents the major biological challenge to provide a viable artificial environment for tissue regeneration. On the scaffold level, cell deposition is known to have a considerable effect on the transportation efficiency in porous constructs [6]. In other words, localized cell proliferation can influence the bio-transportation and thereby affect the global cell vitality; the cells living far away from the oxygen supply may expect an ongoing deterioration of vitality induced by the continual upstream tissue growth and declining oxygen availability [7]. It is commonly recognized that the microscopic architecture and the interconnectivity of porous network play a critical role in regulating nutrient transport and cell distribution [8]. The structural design is therefore a decisive factor in the long term viability of tissue scaffolding.

The fabrication of porous tissue scaffolds and their physical effects on cell growth have been studied extensively in the past [9], where simplistic parameters such as porosity, tortuosity and interconnectivity are commonly used. A range of structural requirements have been established along with the solutions to tackle the various aspects of this biological problem, including pore size for vascularization (> 100 μm) [10], macroscopic porous network for cell migration (~ 100 μm) [2, 3, 11], pore connectivity for mass transport [8], and enhanced diffusion in microporosity (~1 μm) [5]. However, it is often difficult and impractical to standardize scaffold design or to describe the architectures in details in terms of these vague geometric parameters.

Design of micro-architecture for tissue scaffold is also gaining increasing attention recently under the expectation of resolving the nutrient transportation problem in perfusion system, and providing a clear definition of design optimality [8] [12]. Optimal microstructures for criteria ranging from mechanical stiffness, transport effectiveness [13], to properties of fluid dynamics [14] have been under investigation and characterized. These studies have managed to clarify the ideal architecture of porous medium in structural terms, but usually in forms of voxelized model that has limited capability of precisely defining surface features.

To study the effect of microstructure on the mass transportation for the purpose of tissue scaffold design, a better surface tracking method is essential. In this case, the level set method provides a suitable framework for smooth surface modeling by isosurface extraction. This isosurface will not only allow better boundary definition, but also provide an insight into the key boundary features that define the optimality. We hereby propose the combined level set/isosurface technique to determine the optimal scaffold microstructure for mass transport.

4. Methods

The proposed diffusion optimization procedure involved the isosurface modeling, the homogenization of effective diffusivity in porous medium, sensitivity analysis, and the established level set algorithm for topology optimization [15, 16]. The porous structure of tissue scaffolds is subjected to design optimization (Fig. 1). To practically compute the effective diffusivity of oxygen through a porous structure, the homogenization is performed on a representative volume element (RVE) [17, 18] (Fig. 1b) instead of the full-scale model, based on the formulation of effective conductivity [13]. The notion of homogenization herein is to treat the global system as homogenous. The local (microscopic) system on the other hand is assumed to fluctuate in a periodic manner, thus certain relationships can be derived from the periodic boundary conditions to relate the local diffusion behavior to the global transport characteristics. The design optimization of the RVE model is subsequently carried out using the level set method, subjected to the compliance criterion.

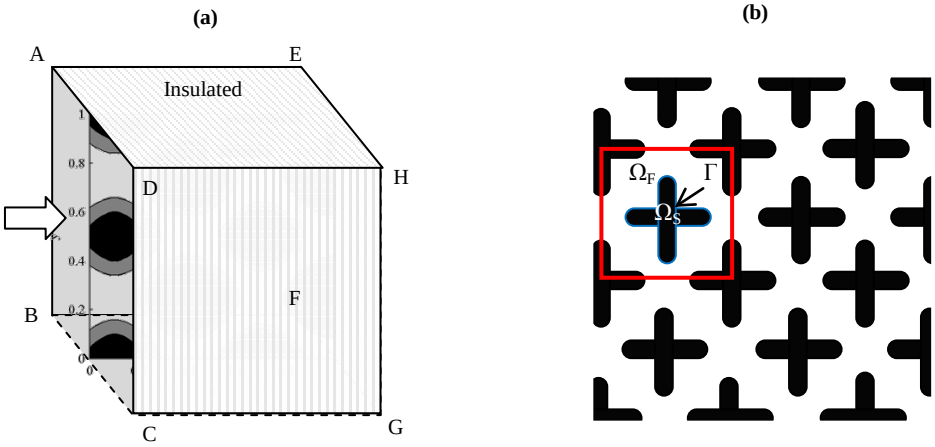

Figure 1: Schematic representation of (a) the one-way diffusion transport through the porous tissue scaffold and (b) the extraction of an RVE model.

A level set is defined as $\Gamma: \varphi(y) = 0$ (Fig. 2). It can be described as a continuous surface that divides the design domain into two sub-domains, namely solid ($\Omega_S: \varphi(y) > 0$) and fluid ($\Omega_F: \varphi(y) < 0$) (Fig. 2b). The objective of this microstructural optimization is to maximize the effective diffusivity J:

$$Maximize: J(y,\varphi) = \int_{\Omega_F} \left(1 - \frac{du}{dy}\right)^T D(\varphi) \left(1 - \frac{du}{dy}\right) \mathrm{d}\Omega$$
$$Subject\ to: \quad \frac{\int \rho(y) dy}{\Delta x} = V_0 \tag{1}$$

where y is the local coordinate, φ is the level set function, and u is the characteristic solution of,

$$\frac{d}{dy}\left[D\left(1 - \frac{du}{dy}\right)\right] = 0 \tag{2}$$

in the microscopic sub-domain Ω_F [19]. The objective function is also the effective diffusivity.

The evolution of a level set model is controlled by the so-called velocity function V, which decides the relative speed of surface movement. The level set function is updated through solving the Hamilton-Jacobi equation:

$$\frac{d\varphi}{dt} + (V + \lambda)|\nabla\varphi| = 0 \tag{13}$$

where dt is the pseudo time step, V is the velocity function, and λ is the Lagrange multiplier for some prescribed volume constraints. In the conventional level set methods, the solid-fluid boundary is not precisely located [14]. V_e is based on the volumetric (elemental) sensitivity but scaled using the delta function, $\delta(\varphi)$:

$$V_e = \delta(\varphi)\left(1 - \frac{du_e}{dy}\right)^T D(\varphi)\left(1 - \frac{du_e}{dy}\right) \tag{4}$$

where the subscript *e* denote elemental result.

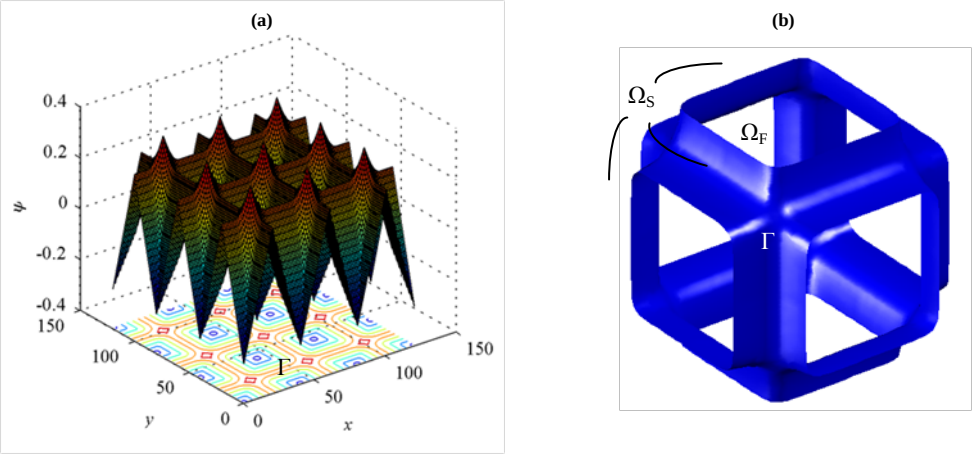

Figure 2: Schematic representation of (a) a level set function and (b) an isosurface of RVE.

In contrast, the velocity function of an isosurface can be interpolated from the elemental results, in which the nodal sensitivity on the actual solid-fluid boundary can be determined using

$$V_n = \sum \left(1 - \frac{du_e}{dy}\right)^T D(\varphi) \left(1 - \frac{du_e}{dy}\right) / l_e \qquad (5)$$

where the subscript *n* denote nodal result and l_e is the distance from individual element centers to the node on the surface. Note that the nodal sensitivity takes the distance-weighted average from all adjacent elements. Similarly, a 3D fixed-grid velocity function can be generated from a distance-weighted interpolation from the surface node to the grid. The 3D matrix of V is then flood-filled with the value of surface velocity. This "body" velocity has no actual effect on topological evolution but helps preserve the smoothness of the level set function, φ. Finally, the Lagrange multiplier is calculated as the integral,

$$\lambda = -\frac{\int_\Gamma V d\Gamma}{\int_\Gamma d\Gamma} \qquad (6)$$

across the solid-fluid boundary Γ.

Boundary constraints can be applied to restrict the isosurface movement. A practical application of the boundary constraint is the reservation of local solid or fluid regions. This is achieved by the conditional scaling of the velocity function: the closer the local surface is to the reserved region, the slower the velocity. The velocity is reduced to zero once the local isosurface makes contact with the regions reserved for particular phases. Hence, further local structural evolution can be prevented. The conditional scaling is only activated if the isosurface is moving directly toward and within a certain distance to those regions.

In this part of procedure, the scaffold RVE was created within a cubic microscopic domain (y), with planar and axial symmetry in all three orthogonal directions. The symmetry and hence, isotropy, was maintained throughout the design evolution by means of numerical operations including matrix mirroring/rotation. The isosurface model was generated from the level set function $\varphi(y)$ to track the exact solid-fluid boundary position more precisely. This modified modeling method replaces the conventional fixed mesh with triangulated surfaces, and the volume Ω_F enclosed by the isosurface was re/meshed every iteration with unstructured tetrahedral elements to create the finite element models. The level set function was initialized as a distance function, in which the value of a point is equal to the distance from this point to its nearest surface.

5. Results and Discussion

Poor cell proliferation in porous tissue scaffolds often occurs as a result of inadequate oxygen supply. This failure is attributed to the inefficient transportation network and the adverse effect of cell deposition and proliferation. To solve this problem, a level set based optimization has been conducted to determine the optimal microstructure for the diffusion transport in tissue scaffold. The periodicity of the microstructure was assumed. To define the solid-fluid boundary more precisely, the microstructures were modeled in form of 3D isosurface in a cubic design domain. The initial fluid domain was created as three intersecting square channels with a total

volume of 50% of the entire design space (Fig. 3a). The homogenization was performed to determine the effective diffusivity. The design evolved according to the compliance criterion.

As shown in Fig. 3, the RVE structure had underwent a significant transformation from the original interconnecting square channels to the uniform gaps (Fig. 3a-e). The evolution involved two major stages: the first stage is the minor shape optimization of the pore interconnection; and the second stage is the major topological transition in which the microscopic model evolved toward the optimal diffusion form. Starting with a basic cubic cell with three orthogonal square channels intersecting at the center of the cube (Fig. 3a), the sharp solid corners and edges at the channel intersection firstly deformed and became smoothened (Fig. 3b). The overall change in shape and the objective function in the first 50 iterations were unremarkable as shown in Fig. 4. Only when the shape became optimal, a shift in the evolution trend occurred and the topology optimization was initiated (iterations 50-100), marking the beginning of the second part of optimization.

The second stage was characterized by the splitting solid phase and the thinning diffusion domain: the surface of flow domain protruded and cut into the solid domain along the x/y/z planes in all orthogonal directions (Fig. 3c and 3d). This protrusion, or cracking from a solid perspective, propagated until the design domain became fully divided into eight isolated blocks in eight corners (Fig. 3e). From a periodic point of view, the initially continuous solid was split into discontinuous blocks. The originally continuous isosurface also broke down into self-enclosed shells with a roughly cubic shape and smooth edges. However, this design cannot be materialized unless some continuity boundary constraint is enforced (Fig. 3f). In that case, the evolution would still follow a similar smoothening-splitting path but without fully dividing the solid domain into isolated isles.

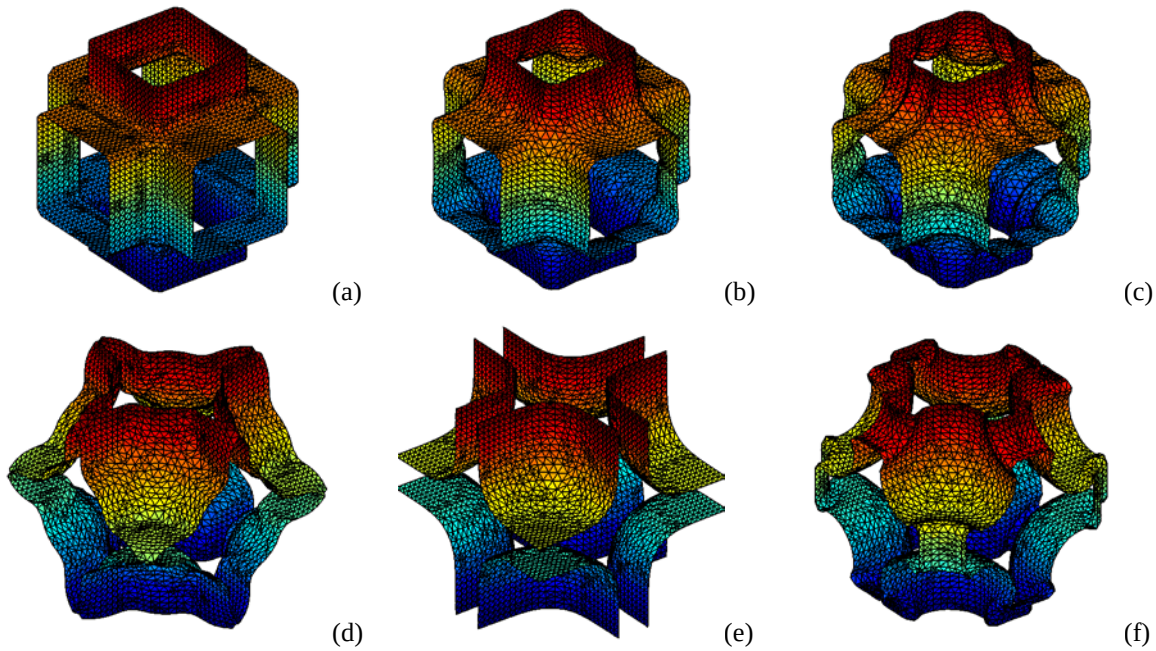

Figure 3. The evolution of RVE model: (a) initial model, (b) 50th iteration, (c) 100th iteration, (d) 200th iteration, (e) 250th iteration, (f) 250th iteration with enforced continuity of solid phase.

The convergence of isosurface model was also a two-stage event in term of the increase in effective diffusivity (Fig. 4). The objective rose by a relatively small amount as the smoothened edges allowed more streamlined diffusion transport. The increase in diffusivity is attributed to the better accessibility of space for mass movement; the functional transport space is less confined to individual channels aligned in the direction of transport. To avoid an early convergence to the local optimum at the end of the shape optimization (around the 50th iteration), the time step size must be kept constant (Eq.(3)). An appropriate step size would ensure the design evolution entered its second stage quickly, which led to a substantial rise in effective diffusivity (iteration > 150). The rise stabilized as the solid domains became fully divided (iteration > 250). Theoretically, the optimal diffusivity could only be achieved without the continuity condition of solid, but for practical reason, the complete separation had to be prevented by means of space constraints that stopped the isosurface from crossing into the regions preserved for solid scaffold (i.e. strut region). The highest objective value attained is roughly 0.40, which reached the H-S upper bound [20].

The key driving force behind the evolution is the maximization of accessibility of physical space. In the initial model, the central conjunction is available for orthogonal diffusion flux in all directions, while individual channels allow flux in certain directions only. The smoothening event slightly increased the effective volume of the central pore, but the functional value of each channel remains restricted. The "splitting" event transforms each channel volume into the gap space, which is accessible to orthogonal diffusive flow in two directions; i.e. it effectively doubles its value for mass transportation (Fig. 3d). The space of central conjunction and the original channels shrink in size but become available for flux in every direction (Fig. 3e). In summary, the design evolution of the RVE is driven by the maximization of shared transportation space. The more accessible a local volume is to flow in different directions, the higher the diffusivity objective. In other words, the optimal 3D diffusion domain is defined as the one with periodic divider space arrangement and smooth conjunction (Fig. 5). These results agree with the findings from a past study [13] [21].

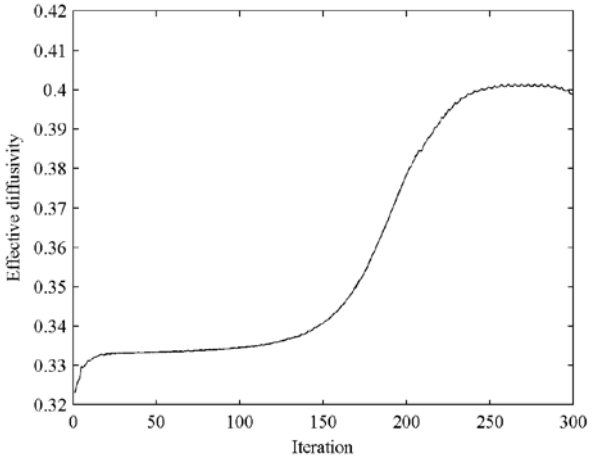

Figure 4. The convergence of the objective function.

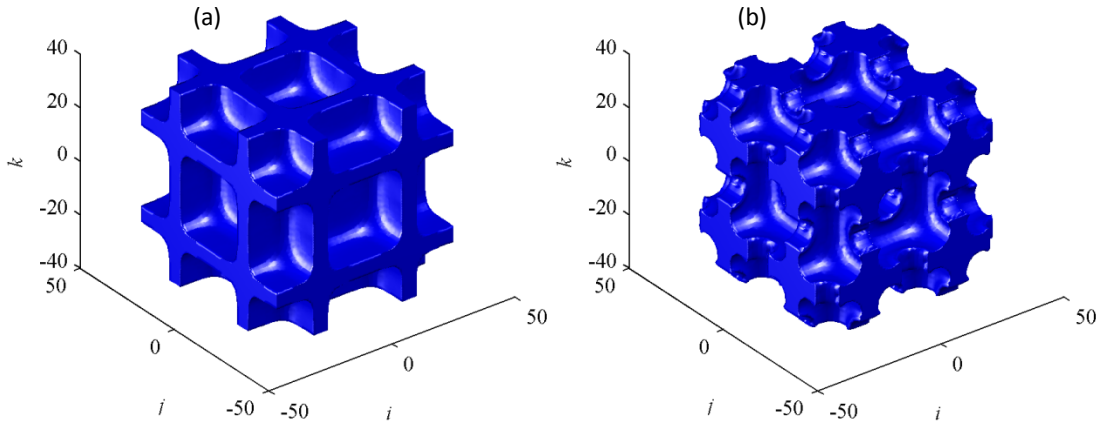

Figure 5. The optimal periodic fluid domain without (a) and with (b) the boundary constraint. In (b), some edge spaces of the RVE boundary are reserved for the solid phase and are impenetrable to isosurface.

The optimal microstructure for diffusion transport has been found through the topology optimization with effective diffusivity criterion. For an *n*-dimensional space, the most volume-effective passage for isotropic diffusivity is an array of (*n*-1)-dimensional spaces. The shape optimization takes place in the mean time can guide the design evolution to a local optimum by smoothening any interconnection. The characteristic solution provides the maximum accessibility to diffusion flow in multiple directions. This result is by no means restricted to the transport in tissue scaffolds, but it can be applied to any common porous structure. However, the validity of the periodicity assumption depends on the uniformity of the actual macroscopic porosity.

6. Conclusion

This study has successfully identified and characterized the optimal microstructure for maximum homogenized diffusivity for tissue scaffold application. On the RVE level, the uniform-width gap space has been identified as

the most volume-effective conduit for diffusion transport, based on the mechanism of space sharing between fluxes in different directions. The implementation of isosurface modeling allows the generation of high quality model and the clear characterization of the optimal topology. The use of boundary constraint enforces the continuity of solid phase. The final result can be practically applied to improve cell vitality in tissue scaffolds.

7. References

[1] F.R. Rose, L.A. Cyster, D.M. Grant, C.A. Scotchford, S.M. Howdle and K.M. Shakesheff, In vitro assessment of cell penetration into porous hydroxyapatite scaffolds with a central aligned channel, *Biomaterials*, 25(24), 5507-14, 2004.

[2] A. Salerno, D. Guarnieri, M. Iannone, S. Zeppetelli, E. Di Maio, S. Iannace and P.A. Netti, Engineered mu-bimodal poly(epsilon-caprolactone) porous scaffold for enhanced hMSC colonization and proliferation, *Acta Biomater*, 5(4), 1082-93, 2009.

[3] M.M. Silva, L.A. Cyster, J.J. Barry, X.B. Yang, R.O. Oreffo, D.M. Grant, C.A. Scotchford, S.M. Howdle, K.M. Shakesheff and F.R. Rose, The effect of anisotropic architecture on cell and tissue infiltration into tissue engineering scaffolds, *Biomaterials*, 27(35), 5909-17, 2006.

[4] S.L. Ishaug, G.M. Crane, M.J. Miller, A.W. Yasko, M.J. Yaszemski and A.G. Mikos, Bone formation by three-dimensional stromal osteoblast culture in biodegradable polymer scaffolds, *J Biomed Mater Res*, 36(1), 17-28, 1997.

[5] B.J. Papenburg, J. Liu, G.A. Higuera, A.M. Barradas, J. de Boer, C.A. van Blitterswijk, M. Wessling and D. Stamatialis, Development and analysis of multi-layer scaffolds for tissue engineering, *Biomaterials*, 30(31), 6228-39, 2009.

[6] T.-Y. Kang, H.-W. Kang, C.M. Hwang, S.J. Lee, J. Park, J.J. Yoo and D.-W. Cho, The realistic prediction of oxygen transport in a tissue-engineered scaffold by introducing time-varying effective diffusion coefficients, *Acta Biomaterialia*, 7(9), 3345-3353, 2011.

[7] J. Malda, T.B. Woodfield, F. van der Vloodt, F.K. Kooy, D.E. Martens, J. Tramper, C.A. van Blitterswijk and J. Riesle, The effect of PEGT/PBT scaffold architecture on oxygen gradients in tissue engineered cartilaginous constructs, *Biomaterials*, 25(26), 5773-80, 2004.

[8] F.P.W. Melchels, A.M.C. Barradas, C.A. van Blitterswijk, J. de Boer, J. Feijen and D.W. Grijpma, Effects of the architecture of tissue engineering scaffolds on cell seeding and culturing, *Acta Biomaterialia*, 6(11), 4208-4217, 2010.

[9] S. Rajagopalan and R.A. Robb, Schwarz meets Schwann: Design and fabrication of biomorphic and durataxic tissue engineering scaffolds, *Medical Image Analysis*, 10(5), 693-712, 2006.

[10] F. Bai, J.K. Zhang, Z. Wang, J.X. Lu, J.A. Chang, J.A. Liu, G.L. Meng and X. Dong, The effect of pore size on tissue ingrowth and neovascularization in porous bioceramics of controlled architecture in vivo, *Biomedical Materials*, 6(1), 2011.

[11] S.H. Oh, I.K. Park, J.M. Kim and J.H. Lee, In vitro and in vivo characteristics of PCL scaffolds with pore size gradient fabricated by a centrifugation method, *Biomaterials*, 28(9), 1664-71, 2007.

[12] F.P.W. Melchels, B. Tonnarelli, A.L. Olivares, I. Martin, D. Lacroix, J. Feijen, D.J. Wendt and D.W. Grijpma, The influence of the scaffold design on the distribution of adhering cells after perfusion cell seeding, *Biomaterials*, 32(11), 2878-2884, 2011.

[13] Y.H. Chen, S.W. Zhou and Q. Li, Computational design for multifunctional microstructural composites, *International Journal of Modern Physics B*, 23(6-7), 1345-1351, 2009.

[14] Y. Chen, S. Zhou, J. Cadman and Q. Li, Design of cellular porous biomaterials for wall shear stress criterion, *Biotechnology and Bioengineering*, 107(4), 737-746, 2010.

[15] S. Zhou and Q. Li, A variational level set method for the topology optimization of steady-state Navier–Stokes flow, *Journal of Computational Physics*, 227(24), 10178-10195, 2008.

[16] M.Y. Wang, X. Wang and D. Guo, A level set method for structural topology optimization, *Computer Methods in Applied Mechanics and Engineering*, 192(1–2), 227-246, 2003.

[17] R. Hill, Elastic properties of reinforced solids: Some theoretical principles, *Journal of the Mechanics and Physics of Solids*, 11(5), 357-372, 1963.

[18] E. Sanchez-Palencia, *Asymptotic Analysis II — Homogenization method for the study of composite media* F. Verhulst, Editor 1983, Springer Berlin / Heidelberg. p. 192-214.

[19] M.P. Bendsøe and N. Kikuchi, Generating optimal topologies in structural design using a homogenization method, *Computer Methods in Applied Mechanics and Engineering*, 71(2), 197-224, 1988.

[20] Z. Hashin and S. Shtrikman, A Variational Approach to the Theory of the Effective Magnetic Permeability of Multiphase Materials, *Journal of Applied Physics*, 33(10), 3125-3131, 1962.

[21] Y. Chen, S. Zhou and Q. Li, Microstructure design of biodegradable scaffold and its effect on tissue regeneration, *Biomaterials*, 32(22), 5003-5014, 2011.